MECSOL 2022 - Proceedings of the 8th International Symposium on Solid Mechanics
M.L. Bittencourt, J. Labaki, L.C.M. Vieira Jr. and E. Mesquita (Editors), Campinas SP, Brazil, October 17th to 19th, 2022

A Radial Basis Function Based Optimization Framework for Variable Axial Composites Materials

Pedro B. Santana[1], Volnei Tita[2,3], Herbert M. Gomes[1], António J.M. Ferreira[3]

[1] Federal University of Rio Grande do Sul, Department of Mechanical Engineering, R. Sarmento Leite, 425, room 202, 2o floor, Porto Alegre, 90050-170, RS, Brazil.
[2] University of Sao Paulo, Sao Carlos School of Engineering, Department of Aeronautical Engineering, Av. João Dagnone, 1100 - Jardim Santa Angelina, 13563-120, Sao Carlos (SP), Brazil
[3] Faculty of Engineering of University of Porto, Department of Mechanical Engineering, Rua Dr. Roberto Frias s/n, 4200-465, Porto, Portugal

This work presents a strategy for the multiobjective optimization variable axial composites. The proposed methodology relies on the integration of three components: a framework for the definition of the orientation of the fiber across the laminate, a structural analysis program, and an optimization algorithm. The optimization design variables are angles values assigned to control points on selected locations over the structure. These control points are used to build a radial basis function(RBF), which describes a smooth fiber pattern. The nodal angles are obtained by evaluating the RBF function values at nodal coordinates. The fibers' orientation at each finite element integration point is determined based on the nodal angles used in conjunction with the shape functions to interpolate angles values to these points. An eight-node degenerated serendipity shell finite element is used for stress analysis. The element formulation takes into account the characteristics of the variable-stiffness laminate. The optimization of the orientation of the fiber is performed using a Multiobjective genetic algorithm (NSGA-II). All components of the optimization framework are implemented in Matlab for the study presented in this work. The methodology is applied to cases where the simultaneous minimization of the stress concentration factor and minimization of the Tsai-Wu failure criterion is desired. The optimum solution obtained by the proposed methodology presents improvements compared to the best unidirectional fiber design, indicating it may be a useful tool for designing variable axial composites.
Keywords: Variable axial composites materials, composite materials, multiobjective optimization, stress analysis, finite element method

INTRODUCTION

According to Pilkey *et al.* (2008), the elementary stress formulas used in the design of structural members are based on the members having a constant section hypothesis or sections with a gradual contour change. This condition is hardly attained in practice due to the presence of shoulders, grooves, holes, keyways, threads, etc., which interrupts stress flow and originates complex stress distributions. Some sites present high stress compared to the surroundings and are known as stress concentration regions.

In a real structure, notches and holes frequently cannot be avoided. As stated by Schijve (2001) the severity of the stress concentration is depending on the geometry of the notch configuration and designers should always try to reduce stress concentrations as much as possible in order to avoid fatigue problems.

Stress concentration in isotropic materials was widely studied, Pilkey *et al.* (2008) presents a wide variety of stress concentration factors for different geometries. However, for composite materials, the literature on the topic is not so vast. Ueng and Lin (1987) uses analytical solutions for a plate with a hole combined with the superposition principle applied to the stress potential functions to develop solutions for plates with two elliptical holes under normal loads. One of the conclusions of this work is that stresses patterns do not change when compared to an isotropic material, but its magnitude does.

Chiang (1998) presents analytical solutions for edge-notched semi-infinite plates using material and shape factors. The shape factor is obtained interpolating two theoretical values of the isotropic material. The solutions obtained are in agreement with the available solution. Weixing and Xinlu (1991) presented one of these solutions, obtained using an eight-node finite element for notched plates made of Borum/Aluminum and Graphite/Epoxy.

The remediation of stress concentration in isotropic materials is done by changing the structure's geometry. In contrast, in composite materials reinforced by continuous fibers, this problem can be addressed by allowing the reinforcement

fibers to assume curvilinear patterns and the changes in geometry. The convenience of such an approach allows the fiber alignment to be parameterized and optimized.

This kind of composite material may be called Variable Axial Composites and many studies have been developed on this theme recently, covering a broad spectrum of objective functions and parameterization methods. Honda *et al.* (2013) parameterize the fibers' configuration using contour lines of a 3rd degree polynomial and assume objective functions for first natural frequency, the Tsai-Wu failure index, and a practicality index (mean curvature). The authors use the NSGA II multiobjective optimization algorithm to generate a Pareto's frontier for the following concurrent objective functions: natural frequencies' maximization $\times$ mean curvature reduction, and Tsai-Wu failure index $\times$mean curvature reduction.

Wu *et al.* (2015) developed a two-level optimization framework using lamination parameters as design variables and critical buckling load as the objective function evaluated by finite element analysis. The lamination parameters are distributed over the plate by B-splines functions, where the convex hull property is exploited to ensure the pointwise feasibility of lamination parameters. Results of plates under compressive loading with different boundary conditions and aspect ratios are presented, and the solutions match well with previously published results.

Aiming at reducing the computational burden, another approach using semi-analytical methods is proposed by Pereira *et al.* (2021). They use a semi-analytical model that combines classical lamination theory (CLT) with the Rayleigh-Ritz method, with fiber angles interpolated by a Lagrange polynomial function of the x and y plate coordinates. Initially, base configurations with unidirectional fibers are assumed, and variations from the higher-order terms of the polynomial are added. The maximization of the first natural frequency and the corresponding damping ratio is sought in that work.

Control points are distributed over the finite element mesh in the present work, and corresponding angle values are assigned. Then, these angles values are interpolated at the integration points using radial basis functions. The Cartesian coordinates of integration points are obtained by transformation from the natural to the Cartesian system using the same element shape functions. A notched plate is selected as an example, which has already been studied with composites reinforced by unidirectional fibers. The objective functions are the stress concentration factor (Kt) and the Tsai-Wu failure index, which are concurrent objective functions. This allows obtaining the Pareto's frontiers. NSGA II algorithm is used, and the results show a considerable improvement for both objective functions.

The novelty in the proposed methodology consists in the combined use of radial basis functions and the finete element's shape functions to obtain variable axial composites numerical model with prescribed fibers directions in the integration points. Another new aspect presented is the potential application of variable axial composites to mitigate stress concentration.

ANALYSIS AND OPTIMIZATION FRAMEWORK

Finite element analysis

For this work, an in-house finite element software was developed using MATLAB (2020). The selected finite element is an eight node degenerated shell finite element proposed by Ahmad *et al.* (1970). In this formulation, the Reissner-Mindlin hypotheses are assumed to be valid: straight lines normal to the reference surface stay straight but not necessarily normal. Another important hypothesis is that the strain energy corresponding to stresses perpendicular to the middle surface is ignored. Accordingly Teixeira-Dias *et al.* (2018), in this way, is indirectly invokes a plane stress state, where thickness variations calculated at the finite element nodes are obtained from normal deformations. The displacements field for this formulation is defined by:

$$\{U^e\} = \begin{Bmatrix} u(\xi,\eta,\zeta) \\ v(\xi,\eta,\zeta) \\ w(\xi,\eta,\zeta) \end{Bmatrix} = \sum_{k=1}^{n_{node}} \begin{bmatrix} N_k & 0 & 0 & -\frac{h_a}{2}\zeta N_k v_{2x}^k & \frac{h_a}{2}\zeta N_k v_{1x}^k \\ 0 & N_k & 0 & -\frac{h_a}{2}\zeta N_k v_{2x}^k & \frac{h_a}{2}\zeta N_k v_{1x}^k \\ 0 & 0 & N_k & -\frac{h_a}{2}\zeta N_k v_{2x}^k & \frac{h_a}{2}\zeta N_k v_{1x}^k \end{bmatrix} \begin{Bmatrix} u_k \\ v_k \\ w_k \\ \alpha_k \\ \beta_k \end{Bmatrix} \quad (1)$$

where N_k represents the shape functions (in this case, 2D isoparametric shape functions), ξ, η and ζ are the natural coordinates, and v_1 and v_2 are components of a vector basis that is used as framework for rotations. The formulation of this basis can be found in Teixeira-Dias *et al.* (2018), Hughes (2000) or Cook (2001).

The strain tensor of each layer is obtained by deriving the displacement field as presented in Eq. (2), where ε_{ii} corresponds to the strain tensor components and u, v, w are the displacement fields in each direction.

$$\left\{\varepsilon_{xx},\varepsilon_{yy},\varepsilon_{zz},\gamma_{xy},\gamma_{xz},\gamma_{yz}\right\}^T = \left\{\frac{\partial u}{\partial x},\quad \frac{\partial v}{\partial x},\quad \frac{\partial w}{\partial z},\quad \frac{\partial u}{\partial y}+\frac{\partial v}{\partial x},\quad \frac{\partial v}{\partial x}+\frac{\partial w}{\partial y},\quad \frac{\partial u}{\partial z}+\frac{\partial w}{\partial x},\right\}^T \quad (2)$$

The element stiffness matrix is assembled as usual:

$$\underset{5NX5N}{[k]} = \int_{-1}^{1}\int_{-1}^{1}\int_{-1} \underset{5NX6}{[B]}^T \underset{6X6}{[E]} \underset{5NX6}{[B]} \quad (3)$$

Where $[E]$ is the material constitutive matrix and $[B]$ is the strain-displacement matrix. The strain field is obtained at the lamina's coordinate system, so it's necessary to transform the $[B]$ matrix from the global to the local coordinate system. This procedure is well described in Teixeira-Dias *et al.* (2018).

To adapt this shell finite element to orthotropic materials, the formulation proposed by Kumar and Palaninathan (1997) is used. In this methodology, the natural variable ζ is explicitly integrated through the assumption that the Jacobian inverse varies linearly along with the thickness.

The stresses are calculated at the integration points and are carried to the nodes by the local least squares smoothing technique presented by Hinton and Campbell (1974).

NSGA-II optimizer

The NSGA-II is a multi-objective genetic algorithm proposed by Deb *et al.* (2002), and it is based on the non-dominated sorting genetic algorithm. The NSGA-II is implemented using a crowded-comparison approach that eliminates the dependence of the solutions' spread of a user-defined parameter and the necessity of comparing each solution with all others. NSGA-II has a good performance for widely distributed Pareto-Optimal solutions. The optimization process starts with generating the initial P0 population by random numbers and applying the non-dominated sorting on each population, being each individual ranked on the dominance relation. After this initial step, individuals within each rank are sorted again based on the crowded-comparison metrics, and the population density is evaluated. This metric allows constructing an intermediate mating pool where individuals are stored based on selection by tournament, resulting in individuals with a high probability of occurrence, better-ranked, and less crowded populations. In this pool, genetic operations generate the child population Qn, which, in conjunction with the population Pn, are used to create an integrated population Rn. After that, fitness values are assigned to all individuals by the non-dominated sorting and by the crowded distance metrics. Finally, an elitist sorting algorithm selects individuals with better fitness, and these become parent individuals Pt+1. The described process is repeated until all generations are computed (n = nmax). In the end, individuals with rank one among the final population are the Pareto optimal solutions.

Radial basis functions and fiber discretization

According to Biancolini (2017) Radial Basis Functions (RBF) consist of a very powerful tool due to their capacity to interpolate at any point of the space a scalar function defined at discrete points giving the exact values at original points. In the proposed method, control points (CP) are distributed over the structure's area of interest and will be assigned fiber angles values. The points' Cartesian coordinates are used as a framework to construct these functions used to interpolate fiber angles at node's coordinates.

The radial basis interpolation function for a given integration point is defined by:

$$\theta_{it}(x_{it},y_{it},z_{it}) = \sum_{i}^{n_{CP}} \gamma_i \phi\left(\left\|\{n\}-\{CP_i\}\right\|\right) + h(n) \quad (4)$$

where θ_{it} is the fiber angle at the integration point it, h_n is a polynomial corrector which is added to guarantee the solvability and uniqueness of the fit, $\{n\}$ is a vector containing the x, y and z coordinates at the integration point it and $\{CP_i\}$ is the coordinates x, y, and z vector of a control point i. Finally, $\{\gamma\}$ is a vector of weights values for radial basis function $\phi(.)$, which, accordingly to Biancolini (2017) accumulates the interactions with all surrounding control points gained computing the radial distance between the coordinate n and each control point, consisting of a transformation $\mathbb{R} \Rightarrow \mathbb{R}$.

Assuming that the basis function is a conditionally positive definite function and a linear polynomial is used, the weights of the RBF interpolator $\{\gamma\}$ and the linear polynomial coefficients $\{\beta\}$ by the solution of the system of equations:

$$\begin{bmatrix} [M] & [P_s] \\ [P_s]^T & [0] \end{bmatrix} \begin{Bmatrix} \{\gamma\} \\ \{\beta\} \end{Bmatrix} = \begin{Bmatrix} \{CP\} \\ \{0\} \end{Bmatrix} \tag{5}$$

where the term $[M]$ is the interpolation matrix defined evaluating all the radial interactions between control points, and $[P_s]$ is a constraint matrix that balances the polynomial contribution.These terms are described in Eq. (6) and Eq. (7).

$$M_{ij} = \Phi(\|\{CP_i\} - \{CP_j\}\|), 1 \leq i \leq 3\,, 1 \leq j \leq 3 \tag{6}$$

$$P_s = \begin{bmatrix} 1 & x_{CP_1} & y_{CP_1} & z_{CP_1} \\ 1 & x_{CP_2} & y_{CP_2} & z_{CP_2} \\ \vdots & \vdots & \vdots & \vdots \\ 1 & x_{CP_{dimension(\{CP_x\})}} & y_{CP_{dimension(\{CP_y\})}} & z_{CP_{dimension(\{CP_z\}))}} \end{bmatrix} \tag{7}$$

The angles are interpolated at node level to the integration point level, increasing the flexibility considerably to construct fibers' patterns. This represents more freedom than just onde fiber angle value at the element's centroid. The fiber angles interpolation at the integration point is done as shown in Eq. (8):

$$\theta_{it} = \sum_{i=1}^{n_{nodes}} N(\xi,\eta)_i \theta_{node_i} \tag{8}$$

The developed finite element software uses a 2×2 Gauss point integration scheme. The selected radial basis functions is the cubic spline $\varphi = r^3$.

NUMERICAL RESULTS

To demonstrate the advantages of the proposed technique, a double notched plate was studied. The assumed objective functions are stress concentration factor K_t and Tsai-Wu failure index minimization. To decrease the Tsai-Wu failure index, one can figure out to reinforce with fibers aligned to the load in the region around the hole or notch, but in doing so, the stress around the hole or notch will also increase in this direction. On the other hand, if the fibers in the region around the hole are placed perpendicular to the load, the stress in the load direction is reduced. Consequently, K_t will also reduce, but the Tsai-Wu failure index will increase. Therefore, these functions are concurrent, and a trade-off can be built using the Pareto frontier obtained by the NSGA-II multiobjective optimization algorithm. The selected optimizer is the NSGA-II algorithm and is selected. Previous trials selected a population of 200 individuals and a maximum of 200 generations based on this problem. The upper and lower bounds for the fiber angles were assumed in the interval $[-\pi, \pi]$.

Equation (9) indicates the Tsai-Wu failure criterion, where X and Y are the failure stresses in this directions and c and t means compression and traction respectively.

$$\Phi = \frac{X_c - X_t}{X_c X_t}\sigma_1 + \frac{Y_c - Y_t}{Y_c Y_t}\sigma_2 + \frac{1}{X_c X_t}\sigma_1^2 + \frac{1}{Y_c Y_t}\sigma_2 + \frac{1}{X_c X_t Y_c Y_t}^{1/2}\sigma_1\sigma_2 + \frac{1}{S^2}\tau_{12} \tag{9}$$

Double notched plate

The structure used for this example is a plate with two notches extracted from Weixing and Xinlu (1991). First, it was tested whether the developed software can reproduce one of the results obtained by the authors. The selected plate is shown in Fig. (1). The plate's has only one layer and is made of a Borum/Aluminum composite with E_1=210 GPa, E_2=132 GPa, v_{yx}=0.22, G_{yx}=44.8 GPa and 5 mm thickness. The used finite element mesh is generated in ANSYS (2016) software and then exported to the developed software. The mesh has 2400 elements and its details are shown in Fig. (1).

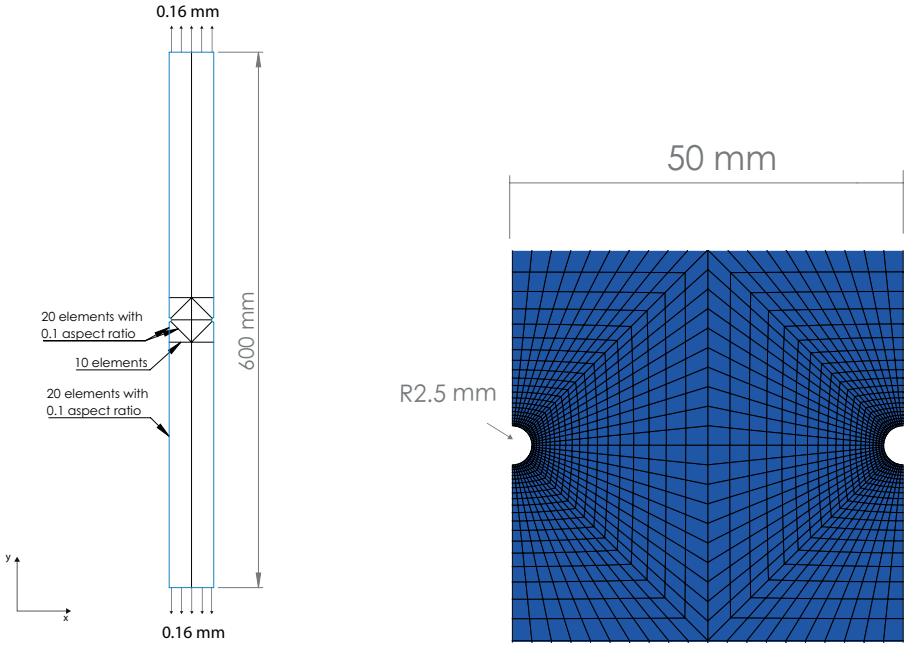

(a) (b)

Figure 1: (a) FE Mesh and notch region detail (b) Precribed region with variable fiber angle.

Prescribed normal displacements of 0.16 mm are imposed at the plate as shown in Fig. (1). According to Weixing and Xinlu (1991) the K_t is obtained dividing the maximum normal stress in direction 1 in the load (or fiber) direction by the nominal normal stress in this same direction $\left(\frac{\sigma_{1_{max}}}{\sigma_{1_{nominal}}}\right)$. The nominal stress is measured at the board of the plate, where the displacements are applied. For the presented plate with the fiber aligned with the displacement direction and discretized with a much coarser mesh, the authors obtained a K_t of 3.6556 while in the present work with the proposed mesh a K_t of 3.6499 is obtained.

Since Weixing and Xinlu (1991) did not present data for the material strength, three materials with data available in Mendonça (2019) are tested. The plate geometry, thickness and prescribed displacements remain unchanged. The material elastic mechanical properties are shown in Tab. 1.

Table 1: Mechanical Properties

Material	E_1 (GPa)	E_2 (GPa)	ν_{12}	G_{12} (GPa)	X_t (MPa)	X_c (MPa)	Y_t (MPa)	Y_c (MPa)	S(MPa)
Scotchply 1002	38.6	8.27	0.26	4.14	1062	610	31	1186	72
T300/N5208	181	10.3	0.28	7.17	1500	1500	40	246	68

Nine control points are assumed uniformly distributed over the plate. Only the elements inside a prescribed area can assume a curvilinear fibers pattern. The remaining have their fiber direction set to parallel the displacement direction. In the neighborhood of the prescribed area, the fiber angles at integration points are also set to follow parallel to the axial direction by a new set of control points. Due to the capacity of radial basis functions to recover exactly scalar fields known at original points, the transition between the fibers' inside the prescribed area to the outside will be smooth since the extra control points angle values are set equal to the ones outside the prescribed area and are used to build the interpolation RBF. The control point distribution over the mesh is shown in Fig. (2).

The von Misses equivalent stress is used to evaluate K_t. This equivalent stress is used in Mohamed Mohamed Makki and Chokri (2017) to compare experimental data to finite element results and presents a good fit for small hole diameters.

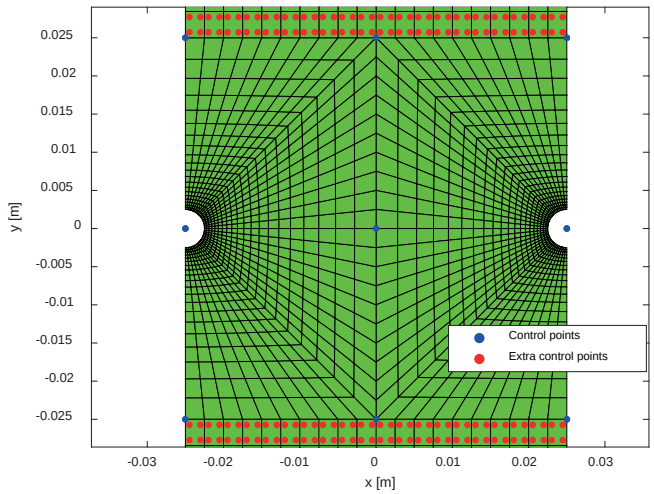

Figure 2: Control points and extra control points with enforced angles.

The obtained Pareto's frontiers are shown in Fig. (3). It's noted that the plate made of T300/N5208 violate the Tsai-Wu failure criterion in all Paretos' frontier points. So, the plate made of Scotchply 1002 has its results detailed. Figure (3) presents all obtained Pareto's frontiers and the numerical results for the Scotchply 1002 plate and a solution for a plate reinforced by unidirectional fibers aligned with displacements direction, this fiber configuration was assumed as reference for comparison with the obtained results.

The obtained K_t and Tsai-Wu failure index results for the patterns highlighted in Fig. (3) are presented in Tab. (2).

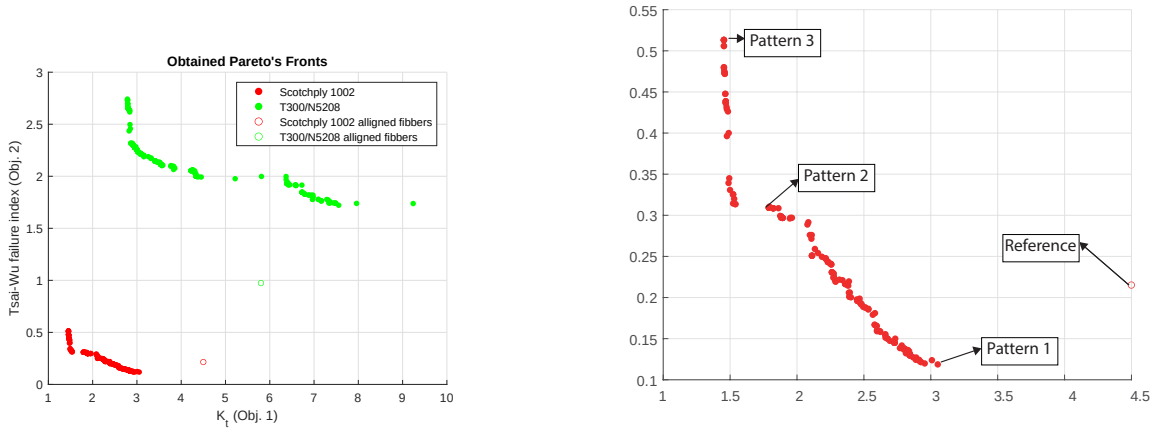

(a) (b)

Figure 3: (a) Pareto frontier. (b) Detail for the Scotchply 1002 and T300/Fiberite plate

Table 2: Obtained results for selected points

	K_t	Tsai-Wu failured index
Reference	4.4988	0.2152
Pattern 1	3.0519	0.1187
Pattern 2	1.7938	0.3106
Pattern 3	1.4535	0.5133

The first pattern reduces the maximum Tsai-Wu failure index by 44.84%, and the second reduces K_t by 32.16% compared to the best unidirectional fiber's pattern (fibers aligned with the displacement direction). The intermediate

pattern increases the Tsai-Wu failure index by 44.33%, and the Kt is reduced by 60.10%, while the last one increases the Tsai-Wu failure index by 138%, and the K_t is reduced by 67.70%.

It is noted that in the first pattern, the fibers assume higher curvatures near the notches than in the plate center, but sufficiently small to let the fibers stay almost tangent to the notches' roots, reinforcing these critical regions against traction loads. Moreover, the fibers near the notches converge to the plate edges at a certain angle, distributing part of the load to the matrix reducing the K_t. In the second pattern, the curvature is more acute, this reduces the fiber's action at the notch root decreasing the structure's resistance in this region, also, the fibers reach the plate edge at higher angles, decreasing the fiber's reinforcement and the normal stress and, consequently, the K_t.

As depicted in Fig. (4), in the last pattern, the fibers reach both the notch hole and the plate edge almost perpendicularly, making most of the load supported by the matrix, and this decreases the Kt factor at the expense of a heavy penalization in strength. In this pattern, the stresses around the notches are severely reduced to approximate the maximum stress on the prescribed area to the remote stress.

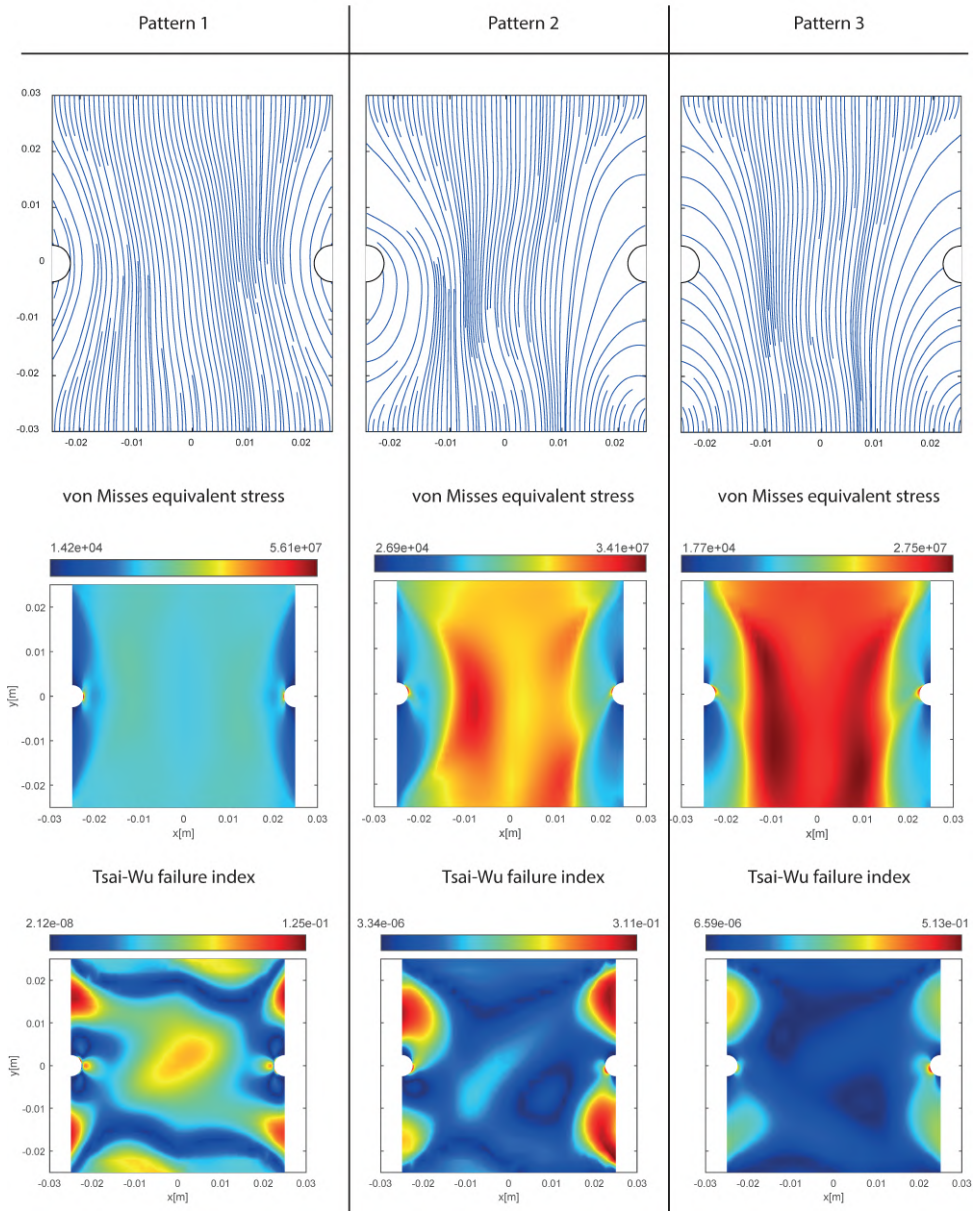

Figure 4: Obtained fibers' patterns, stress distributions and Tsai-Wu failure index distributions for interest area.

CONCLUSION

The proposed methodology has shown the capacity to generate a set of solutions that improve both or just one of the objective functions. The study done with different composite materials has shown that the obtained gains strongly rely on the structures' material and that some of the obtained fiber configurations have shown high complexity, which can lead to difficulties in its production. So, for future works, an index for ease of construction can be considered as other material proprieties like the fibers' density.

The extension of the presented framework to multiple-layer composites using equivalent mechanical properties obtained by homogenization or the 3D evaluation of structures like hollow shafts are also of interest. The optimization of the linear fracture mechanics parameters like the stress intensity factor or Reliability-Based / Robust Based Analysis may also extend the range of applicability of the optimized structure.

ACKNOWLEDGMENTS

Volnei Tita acknowledges the financial support of the National Council for Scientific and Technological Development (CNPq process number: 310656/2018-4), FAPESP-FAPERGS (process number: 2019/15179-2 and 19/2551), and Coordenação de Aperfeiçoamento de Pessoal de Nível Superior – Brasil (CAPES-FCT: AUXPE 88881.467834/2019-01).

Herbert M. Gomes acknowledges the financial support of the National Council for Scientific and Technological Development (CNPq process number: 301719-2017-9 and 304626-2021-0)

REFERENCES

Ahmad, S., Irons, B.M. and Zienkiewicz, O.C., 1970. "Analysis of thick and thin shell structures by curved finite elements". *International Journal for Numerical Methods in Engineering*, Vol. 2, No. 3, pp. 419–451. doi:https://doi.org/10.1002/nme.1620020310.

ANSYS, 2016. *ANSYS Parametric Design Language Guide release 17.0*. ANSYS,Inc, Canonsburg, PA.

Biancolini, M.E., 2017. *Fast Radial Basis Functions for Engineering Applications*. Springer International Publishing : Imprint: Springer, Cham, 1st edition. ISBN 978-3-319-75011-8. doi:10.1007/978-3-319-75011-8.

Chiang, C.R., 1998. "Stress concentration factors of edge-notched orthotropic plates". *The Journal of Strain Analysis for Engineering Design*, Vol. 33, No. 5, pp. 395–398. ISSN 0309-3247, 2041-3130. doi:10.1243/0309324981513093.

Cook, R.D., ed., 2001. *Concepts and applications of finite element analysis*. Wiley, New York, NY, 4th edition. ISBN 978-0-471-35605-9.

Deb, K., Pratap, A., Agarwal, S. and Meyarivan, T., 2002. "A fast and elitist multiobjective genetic algorithm: NSGA-II". *IEEE Transactions on Evolutionary Computation*, Vol. 6, No. 2, pp. 182–197. ISSN 1089778X. doi:10.1109/4235.996017. URL http://ieeexplore.ieee.org/document/996017/.

Hinton, E. and Campbell, J.S., 1974. "Local and global smoothing of discontinuous finite element functions using a least squares method". *International Journal for Numerical Methods in Engineering*, Vol. 8, No. 3, pp. 461–480. ISSN 0029-5981, 1097-0207. doi:10.1002/nme.1620080303. URL https://onlinelibrary.wiley.com/doi/10.1002/nme.1620080303.

Honda, S., Igarashi, T. and Narita, Y., 2013. "Multi-objective optimization of curvilinear fiber shapes for laminated composite plates by using NSGA-II". *Composites Part B: Engineering*, Vol. 45, No. 1, pp. 1071–1078. ISSN 13598368. doi:10.1016/j.compositesb.2012.07.056.

Hughes, T.J.R., 2000. *The finite element method: linear static and dynamic finite element analysis*. Dover Publications, Mineola, NY. ISBN 978-0-486-41181-1.

Kumar, W. and Palaninathan, R., 1997. "Finite element analysis of laminated shells with exact through-thickness integration". *Computers & Structures*, Vol. 63, No. 1, pp. 173–184. ISSN 00457949. doi:10.1016/S0045-7949(96)00297-0.

MATLAB, 2020. *version 9.9.0.1467703 (R2020b)*. The MathWorks Inc., Natick, Massachusetts.

Mendonça, P.d.T.R., 2019. *Materiais Compostos e Estruturas Sanduíche*. Orsa Maggiore, Florianópolis, SC, 2nd edition. ISBN 978-85-907153-2-0.

Mohamed Makki, M. and Chokri, B., 2017. "Experimental, analytical, and finite element study of stress concentration factors for composite materials". *Journal of Composite Materials*, Vol. 51, No. 11, pp. 1583–1594. ISSN 0021-9983, 1530-793X. doi:10.1177/0021998316659915. URL http://journals.sagepub.com/doi/10.1177/0021998316659915.

Pereira, D., Sales, T. and Rade, D., 2021. "Multi-objective frequency and damping optimization of tow-steered composite laminates". *Composite Structures*, Vol. 256, p. 112932. ISSN 02638223. doi:10.1016/j.compstruct.2020.112932.

URL https://linkinghub.elsevier.com/retrieve/pii/S0263822320328580.

Pilkey, W.D., Pilkey, D.F. and Peterson, R.E., 2008. *Peterson's stress concentration factors*. John Wiley, Hoboken, N.J, 3rd edition. ISBN 978-0-470-04824-5. OCLC: ocn175286374.

Schijve, J., 2001. *Fatigue of structures and materials*. Kluwer Academic, Dordrecht ; Boston, MA. ISBN 978-0-7923-7013-0.

Teixeira-Dias, F., Pinho-Da-Cruz, J., Fontes Valente, R.A. and Alves de Sousa, R.J., 2018. *Método dos Elementos Finitos. Técnicas de Simulação Numérica em Engenharia*. ETEP, Lisbon, Portugal. ISBN 978-9728480400.

Ueng, C.E.S. and Lin, J., 1987. "Stress Concentrations in Composite Laminates". *Journal of Engineering Mechanics*, Vol. 113, No. 8, pp. 1181–1193. ISSN 0733-9399, 1943-7889. doi:10.1061/(ASCE)0733-9399(1987)113:8(1181).

Weixing, Y. and Xinlu, Y., 1991. "Stress concentration factor for an orthotropic finite-width plate containing elliptical edge notches". *Composites Science and Technology*, Vol. 41, No. 1, pp. 47–53. ISSN 02663538. doi:10.1016/0266-3538(91)90051-P. URL https://linkinghub.elsevier.com/retrieve/pii/026635389190051P.

Wu, Z., Raju, G. and Weaver, P.M., 2015. "Framework for the Buckling Optimization of Variable-Angle Tow Composite Plates". *AIAA Journal*, Vol. 53, No. 12, pp. 3788–3804. ISSN 0001-1452, 1533-385X. doi:10.2514/1.J054029.

RESPONSIBILITY NOTICE

The author(s) is (are) the only party(ies) responsible for the printed material included in this paper.